NJC

Accepted Manuscript

This is an *Accepted Manuscript*, which has been through the Royal Society of Chemistry peer review process and has been accepted for publication.

Accepted Manuscripts are published online shortly after acceptance, before technical editing, formatting and proof reading. Using this free service, authors can make their results available to the community, in citable form, before we publish the edited article. We will replace this *Accepted Manuscript* with the edited and formatted *Advance Article* as soon as it is available.

You can find more information about *Accepted Manuscripts* in the Information for Authors.

Please note that technical editing may introduce minor changes to the text and/or graphics, which may alter content. The journal's standard Terms & Conditions and the Ethical guidelines still apply. In no event shall the Royal Society of Chemistry be held responsible for any errors or omissions in this *Accepted Manuscript* or any consequences arising from the use of any information it contains.

ROYAL SOCIETY OF CHEMISTRY

www.rsc.org/njc

New Journal of Chemistry

ARTICLE

Magnetic nanoparticles based dispersive micro-solid-phase extraction for the determination of malachite green in water samples: Optimized experimental design

Received 03th July 2015,
Accepted 28th September 2015

DOI: 10.1039/x0xx00000x

www.rsc.org/

Arash Asfaram, [a] Mehrorang Ghaedi, [*a] Alireza Goudarzi, [b] Mustafa soylak, [c] and Sanaz Mehdizadeh Langroodi [d]

The paper presents an extraction method based on dispersive-nanoparticles-solid phase microextraction (DNSPME) for preliminary preconcentration and subsequent spectrophotometric determination of trace amounts of malachite green (MG). The nanoparticle application permit easy separation and extraction of MG from trout fish water and natural water samples. The analyte was accumulated on γ-Fe_2O_3 nanomaterial loaded on activated carbon (γ-Fe_2O_3-NPs-AC) that identified by FESEM, XRD, FTIR, EDS and UV-Vis techniques. The influence of expectable parameters on extraction recovery according to $p < 0.05$ was intrestigated and judged using two-level Plackett-Burman screening design with 7 variables (adsorbent mass, centrifugation time, eluent volume, ionic strength, pH, ultrasonic temperature and ultrasonic time). It was found that three significant variables named adsorbent mass, eluent volume and pH has great influence that for optimized using central composite design combined with desirability function. Results showed that semi-empirical obtained second-order model efficiently were able to predict ER% MG adequately with coefficient of determination of 99.7% ($p < 0.001$) the higher efficiency of model was revalued by good compromise between experimental and predicted data. Working under optimum conditions specified as 0.6 mg of adsorbent, 120 µL of eluent volume at pH 6.0 lead to achievement of high and reasonable linear range over 1-4000 ng mL^{-1} (R^2=0.999) with detection limits of 0.175 ng mL^{-1} and the obtained quantification limits of 0.583 ng mL^{-1}. The relative standard deviations (RSDs) for ten replicate were less than 3.50%. The proposed method was successfully applied for the determination of MG in trout fish water and natural water samples with excellent recoveries correspond to spike samples. All these results proof the suitability of present method in term of simplicity, easy operation condition, efficiently and sensitivity for the determination of MG in real samples.

1. Introduction

Malachite green (MG) is a cationic assign to triphenylmethane group in aquaculture industry as anti-fungal, anti-microbial and anti-parasitic agent, because of its relatively low price and good efficacy in the prevention and treatment.[1-3]

MG and its metabolite leucomalachite green to cause mutagenesis and human carcinogenesis [4] that limit its application in aquaculture European Union and US FDA efficiency lead to its.[5] Therefore, it is very important to develop sensitive detection methods for MG determination and its metabolites in foodstuffs such as fish samples. Most analytical protocols for MG determination based on mass spectrometry (MS), liquid chromatography (LC) in combination with triple quadruple,[3, 6-8] high performance liquid chromatographic (HPLC) [9-12] and other methods such as electro-chemi-luminescence (ELC),[13] spectrophotometric[14-16] has been reported application of low coast and even accessible. The accuracy for quantification of MG has been improved by UV-Vis combined with solid-phase microextraction (SPME) that performing preliminary. The analysis of MG in food samples is chillingly point pre-treatment stages is required to conduct food residue analysis. SPME applicability in various sample matrixes is supplied from its advantages viz. high enrichment factor, rapid phase separation, low consumption of organic solvents and cheap coast and ability of application as on-line or off-line mode.[17-19] The unique and critical

[a] Chemistry Department, Yasouj University, Yasouj 75918-74831, Iran. E-mail address: m_ghaedi@mail.yu.ac.ir; Tel: +98 741 2223048; fax: +98 741 2223048.
[b] Department of Polymer Engineering, Golestan University, Gorgan, 49188-88369, Iran
[c] Erciyes University, Fen Fakultesi, Department of Chemistry, 38039 Kayseri, Turkey
[d] Department of Chemistry, Golestan University, Gorgan, 49138-15759, Iran

in such protocol is best selection of sorbent to achieve good recovery and high enrichment factor.

SPE based on reversible sorbents such as graphene,[11] diatomite,[15] monolithic fiber [20] and molecularly imprinted polymer, [13, 21] were used to enrich the MG and possible its accurate and precise monitoring in various real samples.

The extensive application of nano-scale material is related their unique properties like high adsorption capacity, fast mass transfer and high surface area to mass ratio, can differ from those in the micro and macro world and even depend not only on the chemical composition and phase but also on the size of the given materials.[22] Knowledge and search did not show any magnetic nanoparticles composite application MG preconcentration.[17]

Magnetic metal oxides based on cubic spinel structured magnetite (γ-Fe_2O_3) is best production of magnetic materials applicable [23, 24] at nano scale source for in electronics, catalysis and biomedical engineering. So simple ferric oxide (γ-Fe_2O_3) was low price, high air stability and low toxicity which simply via precipitation can be produced is wide application nano-scale magnetic material. [25]

RSM is a statistical method that uses quantitative data from appropriate experiments to determine regression model and operating conditions.[26] RSM is basically used for process development and optimization. It helps in evaluating the relative significance of the variables that influence the process.[27]

In this technique the different groups of designs such as Plackett–Burman design (PBD) was used and introduced in Plackett and Burman.[28] Central Composite Design (CCD) was used for determine and estimation of effect of variables and their interaction.[27, 29]

Therefore, the aim of the present study was to investigate the potential of applicability of γ-Fe_2O_3 nanoparticles loaded on activated carbon (AC) (γ-Fe_2O_3-NPs-AC) for the extraction and preconcentration of MG in trout fish water and water samples. In this method, nanoparticles are dispersed in aqueous media by ultrasonic were to accelerate analyte sorption and in later stages all accumulate analyte is eluted by acetonitrile and determined by UV-Vis spectroscopy. Dispersive nano-solid phase micro-extraction (DNSPME) as novel method possess advantages viz. fast operation, simple, high sensitivity, low limit of detection and high linear range that candidate this protocol for usage in MG quantification in real samples with complication materials. The experimental variables such as adsorbent mass, centrifuge time, eluent volume, ionic strength, pH, ultrasonic temperature and time were optimized by PBD for screening and CCD for optimizing the significant factors. The developed procedure for successfully were applied for MG determination in trout fish water and water samples.

2. Experimental

2.1. Reagents and materials

All chemicals including hydrochloric acid (HCl), sodium hydroxide (NaOH), sodium chloride (NaCl), sulfuric acid (H_2SO_4) and acetonitrile (CH_3CN) with the highest purity available are purchased from Merck (Dermasdat, Germany). Iron (II) sulfate heptahydrate ($FeSO_4$, $7H_2O$) and ammonium iron (III) sulfate dodecahydrate (NH_4Fe $(SO_4)_2.12H_2O$) were purchased from Sigma company. Malachite green (MG) dye (Sigma–Aldrich) has following information (a) CAS number: 569-64-2, (b) color index number: 42000, (c) molecular weight: 364.91 g mol^{-1}, (d) empirical formula: $C_{23}H_{25}ClN_2$ and (e) λ_{max}: 617 nm. The MG stock solution (100 mg L^{-1}) was prepared by dissolving 10 mg of solid dye in 100 mL with double distilled/deionized water (produced by a Milli-Q system (Millipore, Bedford, MA, USA) and the working concentrations daily were prepared by its suitable dilution.

2.2. Instrumentation

A UV–Vis spectrophotometer (model V-530, Jasco, Japan) with two 1 cm glass cells and scan speed of 1000 nm/min was used for absorbance measurements. The morphology of the nanoparticles were observed by field emission scanning electron microscopy (FE-SEM: Hitachi S4160, Japan) under an acceleration voltage of 15 KV. X- ray diffraction (XRD, Phillips, PW 1800) was performed to characterize the phase and structure of the prepared nanoparticles using $Cu_{k\alpha}$ radiation (40 KV and 40 mA) at angles ranging from 20 to 80°. The atomic composition of the γ-Fe_2O_3-NPs-AC was analyzed by energy-dispersive X-ray spectrometer (EDS) using an Oxford INCA II energy solid state detector. To investigate the purity as well as the presence of organic and/or other compounds in the prepared nanoparticles, a Fourier transform infrared (FT-IR) spectrum was recorded using a Perkin Elmer-Spectrum spectrometer (RX-IFTIR, USA) in the range of 300–4000 cm^{-1}. Ultrasonic device (TECNO-GAZ, 60 Hz, 130 W, Parma, Italy) is equipped with digital timer and temperature controller. A HERMLE bench centrifuge (2206A, Germany) was used to accelerate the phase separation. A digital pH meter (Ino Lab pH 730, Germany) pH meter was used to measure the pH. The STATISTICA, a statistical package software version 10.0 (Stat Soft Inc., Tulsa, USA) was used for experimental design analysis and subsequent regression analysis of the experimental data.

2.3. Synthesis of nanoparticles

The reaction solution for loading γ-Fe_2O_3 nanoparticles on activated carbon (AC) was prepared as follows: 5.0 g iron (ii) sulfate and 10 g NH_4Fe $(SO_4)_2.12H_2O$ was dissolved in deionized water using 6 mL concentrated sulfuric acid solution. Then, deionized water was added to the solution to make a total volume of 150 mL. Subsequently, 20.0 g AC was added to the prepared solution in an Erlenmeyer flask. Then, 140 mL of 1.5 mol L^{-1} sodium hydroxide was added above mixture drop-by-drop during 70 min along with strong stirring at room temperature and held for 17 h. After 17 h, 100 mL of 3 mol L^{-1} of sodium hydroxide solution was added to the reaction solution drop-by-drop during 40 min at room temperature and stirred strongly for 4 h at room temperature. The obtained γ-Fe_2O_3-NPs-AC were filtered and washed several times by distilled water and dried at 35 °C for 15 h and finally used as an absorbent.

2.4. Recommended procedure

The following steps were applied to adsorb MG onto γ-Fe_2O_3-NPs-AC from the sample solution: 0.6 mg of sorbent was added to 10.0

mL of 0.6 mg L^{-1} analyte solution and its pH was adjusted at 6.0. Subsequently, the mixture solution ultrasonically stirred for 3.0 min The extracted analytes is finally separated from the sample matrix by centrifugation (3000 rpm, 4 min) and subsequently was discarded using a Pasteur pipette. The extracted analytes were eluted with 120 µL of acetonitrile (eluent solvent) following centrifuge for 4.0 min. Finally, 50 µL of the separated phase was drawn out by a Hamilton syringe and directly placed in a micro cell at room temperature and allowed to complete the extraction process.

for analysis of total MG by UV–Vis spectrophotometer at 617 nm. The described procedure was successfully applied for the recovery and determination of MG in various trout fish water and water samples. Schematic diagram of present DNSPME method is shown in Fig. 1.

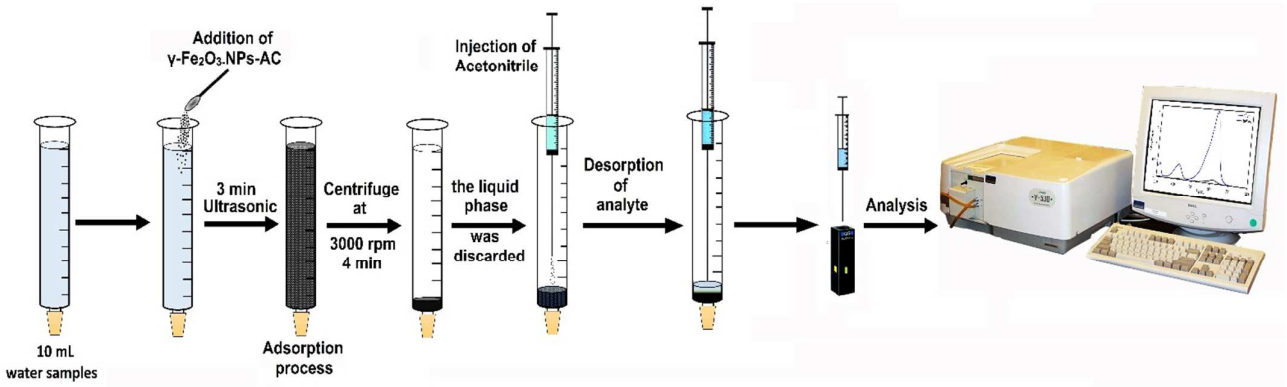

Fig. 1. Schematic diagram of the DNSPME procedure.

2.5. Calculation of extraction recovery and enrichment factor

The enrichment factor (EF) as ratio of concentration of target analytes in sediment phase (C_{sed}) to initial analyte concentration (C_0). C_{sed} was calculated from the calibration obtained from the direct analysis (without preconcentration):[30, 31]

$$EF = \frac{C_{sed}}{C_0} \quad (1)$$

The ER% (analytical response) was calculated as:

$$ER\% = \frac{C_{sed} \times V_{sed}}{C_0 \times V_{aq}} \times 100\% = EF \times \frac{V_{sed}}{V_{aq}} \quad (2)$$

where V_{sed} and V_{aq} are the volume of the sediment phase (acetonitrile) and initial sample solution (10 mL), respectively.

2.6. Experimental design

Response surface methodology (RSM) is convenient and suitable optimization approach composed of various classification like Plackett–Burman design, the Box–Behnken design and the Central Composite Design. The classification about significancy of on ER% was undertaken by Plackett–Burman (PB) design based on n+1 for n variables at two level (-1 for low level, +1 for high level) and 0 for center level.[32] As shown in Table 1, a 2^{7-4} P–B design was applied for eight trials composed of three central points estimation of the experimental error (pure error).[33] Plackett–Burman experimental design is based on the first order polynomial model:[28]

$$y = \beta_0 \sum_{i=1}^{k} b_i x_i \quad (3)$$

Y = the response (extraction recovery), β_0 = model intercept, b_i = linear coefficient, x_i = level of the independent variable, and k = number of involved variables.

The obtained effective variable on the efficiency of DNSPME procedure were optimized by using a central composite design (CCD) and a quadratic model was built between the dependent and independent variables.

The relation of DNSPME efficiency with constructed among, including the adsorbent mass (X_1), Eluent volume (X_2) and pH (X_3) were optimized by CCD at experimental points located in Table 2 at 5 levels including α, -α (axial points), +1, 1 (factorial points) and 0 (central point) and α-value of the used design was 1.682.[28]

The total number of design point needed (N) is determined by the following equation:[34]

$$N = 2^k + 2k + C_p \quad (4)$$

where k is the number of variables and C_p is the number of center point. The required number of experiments for estimation of three process parameters was 17 experiments of which 2^3 experiments were referred to the factorial points.

Table. 1 Factors, codes, low and high levels in 2^{7-4} Plackett–Burman design matrix.

Factors	Levels		
	Low (-1)	Central (0)	High (+1)
A-Ultrasonic temperature (°C)	15.00	25.00	35.00
B-pH	2.00	6.00	10.00

C-Ionic strength (NaCl concentration) (mol L^{-1})	0.00	0.01	0.02
D-Centrifugation time (min)	2.00	4.00	6.00
E-Eluent volume (µL) (Acetonitrile)	100.00	200.00	300.00
F- Ultrasonic time (min)	1.00	3.00	5.00
G-Adsorbent mass (mg) (γ-Fe_2O_3-NPs-AC)	0.80	1.60	2.40

	Factors							ER%	
Run	A	B	C	D	E	F	G	Observed[a] values	Predicted[b] values
1 (C)	25.00	6.00	0.01	4.00	200.00	3.00	1.60	73.32	74.27
2	35.00	2.00	0.00	2.00	100.00	5.00	2.40	77.87	77.55
3	15.00	10.00	0.00	2.00	300.00	1.00	2.40	61.26	60.94
4	15.00	2.00	0.00	6.00	300.00	5.00	0.80	78.19	77.87
5	35.00	10.00	0.02	6.00	300.00	5.00	2.40	63.33	63.01
6	35.00	10.00	0.00	6.00	100.00	1.00	0.80	78.92	78.60
7 (C)	25.00	6.00	0.01	4.00	200.00	3.00	1.60	72.69	74.27
8	15.00	10.00	0.02	2.00	100.00	5.00	0.80	85.03	84.71
9	15.00	2.00	0.02	6.00	100.00	1.00	2.40	74.69	74.37
10	35.00	2.00	0.02	2.00	300.00	1.00	0.80	77.44	77.12

[a] Experimental values of response.
[b] Predicted values of response by RSM proposed model. C: Center Point

Table. 2 Design matrix for the 2^3 central composite design.

Factors	Levels				
	-α	Low (-1)	Center (0)	High (+1)	+α
(X_1) Adsorbent mass (mg)	0.459	0.800	1.300	1.800	2.141
(X_2) Eluent volume (µL)	65.910	100.000	150.000	200.000	234.090
(X_3) pH	3.477	4.500	6.000	7.500	8.523

	Factors			ER% MG		
Run	X_1	X_2	X_3	Observed[a] values	Predicted[b] values	Residual
1	0.800	100.000	4.500	88.450	88.386	0.064
2	1.800	100.000	4.500	29.650	29.243	0.407
3	0.800	200.000	4.500	66.650	66.143	0.507
4	1.800	200.000	4.500	32.560	33.825	-1.265
5	0.800	100.000	7.500	85.430	83.324	2.106
6	1.800	100.000	7.500	56.550	56.216	0.334
7	0.800	200.000	7.500	74.450	74.016	0.434
8	1.800	200.000	7.500	74.510	73.733	0.777
9	0.459	150.000	6.000	97.146	98.591	-1.445
10	2.141	150.000	6.000	48.876	48.620	0.256
11	1.300	65.910	6.000	48.080	49.405	-1.325
12	1.300	234.090	6.000	45.567	45.431	0.136
13	1.300	150.000	3.477	56.020	55.444	0.576
14	1.300	150.000	8.523	82.980	84.745	-1.765
15 (C)	1.300	150.000	6.000	74.345	73.520	0.825
16 (C)	1.300	150.000	6.000	72.965	73.520	-0.555
17 (C)	1.300	150.000	6.000	73.453	73.520	-0.067

[a] Experimental values of response.
[b] Predicted values of response by RSM proposed model.
C: Center Point

The set of axial points included 2×3 experiments, while other experiments were referred to the repeated experiment of central point. The central point (C_p) was repeated 3 times in the aim of experiment precision improvement. Based on the results of the performed experiments the second order polynomial equation was obtained as shown in the following equation: [27, 35]

$$y = \beta_0 + \sum_{i=1}^{3}\beta_i x_i + \sum_{i=1}^{3}\sum_{j=1}^{3}\beta_{ij} x_i x_j + \sum_{i=1}^{3}\beta_{ii} x_i^2 + \varepsilon \qquad (5)$$

y is response variable (ER%), β_0, β_i, β_{ii} and β_{ij} are coefficient of interception, coefficient of linear effect, coefficient of the quadratic effect and coefficient of interaction effect, respectively. ε is the random error accounting for the discrepancies or uncertainties between predicted and observed values. Analysis of variance (ANOVA) was conducted to determine the significance of model and regression coefficients. The applicability of polynomial equation was judged by determination coefficient (R^2), while its credit checked by Fischer's *F*-test and regression coefficients validity assessed by Student's *t*-test. The response surface and contour plots of the model-predicted responses were utilized to assess the interactive relationships between the significant variables.

3. Results and discussion

3.1. Characterization of adsorbent

The absorption spectrum of the prepared γ-Fe_2O_3-NPs-AC (Fig. 2A) was depicted and correspondingly the band gap of γ-Fe_2O_3-NPs-AC was estimated based on following traditional equation and well known constants:[36]

$$(\alpha h\nu)^2 = k\,(h\nu - E_g) \qquad (6)$$

where E_g is the band gap energy, k is a constant, and n is a constant equal to 1 or 4 for direct and indirect band gap materials, respectively. A plot of $(\alpha h\upsilon)^2$ versus hυ (Fig. 2A) is linear at the absorption edge and proof its direct nature. The calculated band gap energy (Eg) (2.20 eV) based on extrapolation of the straight-line portion of the $(\alpha h\upsilon)^2$ vs. hυ plot is larger than that of the bulk γ-Fe_2O_3 (2. 0 eV) attributed to quantum size effects in nano size materials.[37]

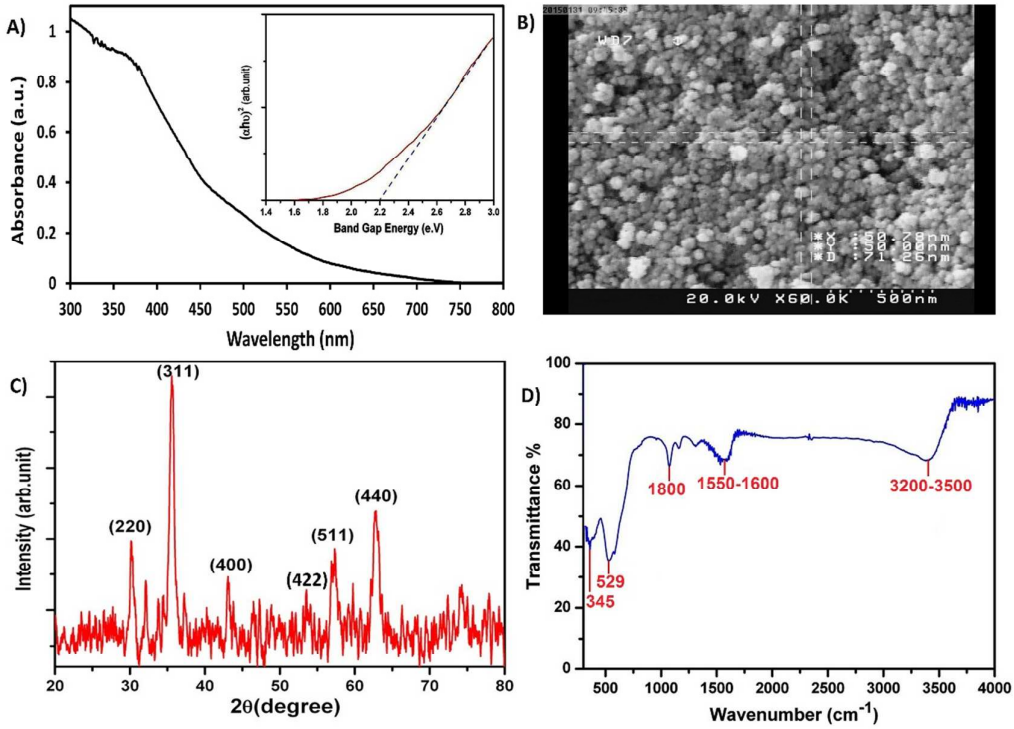

Fig. 2. A) Uv-Vis. absorbance spectrum and Plot of $(\alpha h\nu)^2$ vs. (hυ), B) FE-SEM image, C) XRD pattern and D) FT-IR transmittance spectrum of the prepared γ-Fe_2O_3-NPs.

The FE-SEM image of the prepared γ-Fe_2O_3-NPs (Fig. 2B) confirm its fine and homogenous shape and the size of the particles spherical particles with diameters less than 50 nm.

The structural analysis of the γ-Fe_2O_3-NPs X-ray diffractometer (XRD) (Fig. 2C) show strong XRD peaks at 2θ = 30.1, 35.7, 53.1, 57.1 and 62.7° related to the lattice planes of (220), (311), (422), (511) and (440) confirm the cubic structure of γ-Fe_2O_3 nanoparticles. (JCPDS, No.04-0755), respectively. The observed strong XRD peaks (Fig. 2C) proof well-crystalized structure of the prepared γ-Fe_2O_3-NPs without peaks related to impurities such as Fe, Fe $(OH)_2$, $Fe(OH)_3$ and/or other compounds. The nanocrystalline size of the prepared γ-Fe_2O_3 particles was estimated to be about 13 nm based on application of Debye–Scherrer formula to the full width at half-maximum (FWHM) of the (311) peak.[38, 39]

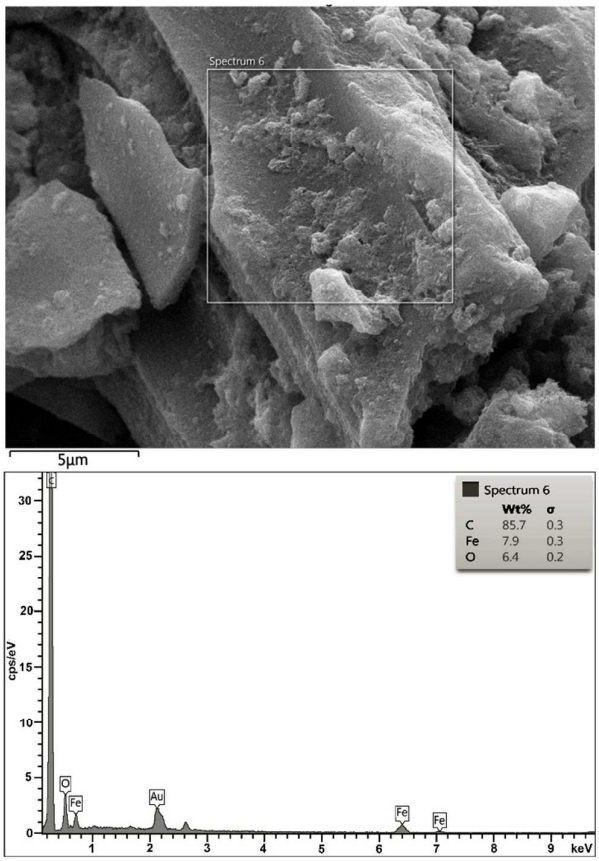

Fig. 3. EDS analysis of the γ-Fe_2O_3-NPs loaded on activated carbon adsorbent.

The FT-IR spectrum of the prepared γ-Fe_2O_3-NPs (Fig. 2D, 300–4000 cm^{-1}) show presence of broad absorption bonds at 345 cm^{-1} and 529 cm^{-1} assigned to Fe-O bending and stretching vibration modes in γ-Fe_2O_3-NPs, respectively.[40] The observed peaks in the range of 1500-3500 cm^{-1} probably is due to water molecules in the KBr matrix. The observed peak at 1100 cm^{-1} may be due to vibrational mode of the absorbed CO_2 on surface γ-Fe_2O_3-NPs. The FT-IR data do not show that γ-Fe_2O_3 nanoparticles were contaminated by foreign materials.

The chemical composition of the γ-Fe_2O_3-NPs loaded on AC was studied by EDS analysis and confirmed the presence of Fe and O in the sample (Fig. 3). The Au peak is related to the signal detected from gold coating by sputtering during FE-SEM sample preparation. In EDS analysis (Fig. 3), C, O and Fe are the dominant elements throughout the surface of the γ-Fe_2O_3-NPs-AC with weight percentages of 85.70%, 6.40% and 7.90%, respectively.

3.2. Plackett–Burman design (P–B)

-was adopted for the ER%. The significant variables were as follows: adsorbent mass, eluent volume and pH, each of which was assessed at five coded levels (-1.682 (lowest), -1 (low), 0 (center), +1 (high), and +1.682 (highest)), according to Table 2.

Table. 3 Lack of Fit Tests and Model Summary Statistics.

The significant variable with more contribution on the response of the ER% at 95% confidence level justified by mean results obtained by means of Pareto charts (Fig. 4). The length of the bars in such estimation is proportional to the absolute value of the estimated effects. The dashed line represents 95% (P=0.05) of the confidence interval that cross this line are significant values with respect to the response. Each bar has a numerical value that also indicates the magnitude and whether the factor has a positive or negative effect on the response. Fig. 4 represents the results obtained for ER% MG. A negative or positive effect was obtained for seven investigated, while factors, the sorbent mass has most influence on response for, followed by the eluent volume and pH. Accordingly, the ultrasonic, centrifuge time, ionic strength and ultrasonic temperature, had no significant effect on the extraction efficiency that consequently eliminated from further study. At all further stages were selected at 3 and 4 min, 0.01 mol L^{-1} and 25 ºC for ultrasonic time, centrifugation time, ionic strength and ultrasonic temperature, respectively. On the other hand, the adsorbent mass (γ-Fe_2O_3-NPs-AC), eluent volume and pH as significant parameters was examined to achieve maximum efficiency. Thus, different amount of sorbent mass (0.5-2.14 mg) were assayed using volumes of acetonitrile from 66 to 235 µL at pH from 3.5-8.5.

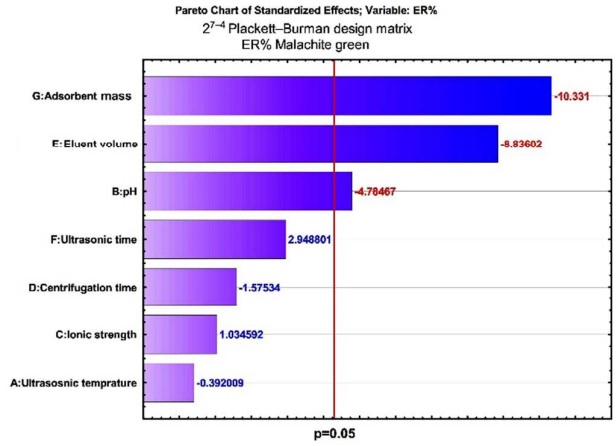

Fig. 4. Standardized main effect Pareto chart for the Plackett–Burman design of screening experiment. Vertical line in the chart defines 95% confidence level.

3.3. Central composite design (CCD)

The next step, in the MG recovery was to searching optimum levels of significant variables. For this purpose, the response surface methodology (RSM) combined with central composite design (CCD)

The quadratic regression model was developed in terms of process variables in coded values (Eq. (5)). Quadratic model was selected for model development as suggested by the software (see Table 3).

Lack of Fit Tests

Source	Sum of Squares	df	Mean Square	F Value	p-value	
Linear	2035.477	11	185.043	377.870	0.003	
2FI	1078.909	8	134.864	275.400	0.004	
Quadratic	14.757	5	2.951	6.027	0.148	Suggested
Cubic	3.549	1	3.549	7.248	0.115	Aliased
Pure Error	0.979	2	0.490			

Model Summary Statistics

Source	Std. Dev.	R^2	Adjusted -R^2	Predicted-R^2	PRESS	
Linear	12.516	0.666	0.590	0.396	3687.659	
2FI	10.392	0.823	0.717	0.669	2023.884	
Quadratic	1.499	0.997	0.994	0.981	117.699	Suggested
Cubic	1.229	0.999	0.996	0.871	786.147	Aliased

Quadratic Model			
Response	CV%	Adequate precision	Mean
ER% MG	2.301	60.304	65.160

Table .4 Analysis of variance table for Quadratic Model.

Source	Sum of Squares	Df	Mean Square	F-value	p-value	
Model	6090.392	9	676.710	301.0175	< 0.0001	significant
X_1	3014.194	1	3014.194	6155.168	0.000162	
X_1^2	0.010	1	0.010	0.021	0.897455	
X_2	19.066	1	19.066	38.934	0.024736	
X_2^2	960.060	1	960.060	1960.501	0.000510	
X_3	1036.412	1	1036.412	2116.417	0.000472	
X_3^2	16.531	1	16.531	33.757	0.028369	
X_1X_2	359.790	1	359.790	734.714	0.001358	
X_1X_3	513.121	1	513.121	1047.824	0.000953	
X_2X_3	83.657	1	83.657	170.833	0.005803	
Lack of Fit	14.757	5	2.951	6.027	0.148407	not significant
Pure Error	0.979	2	0.490			
Cor Total	6106.129	16				

The MG minimum and maximum ER% was found between 29.243% and 98.591%. The positive sign of the coefficients in Eq. (7) indicates the synergistic effect, whereas negative sign suggests antagonistic effect. It is clear from Eq. (7) that individual operating variables adsorbent mass and pH have net negative effect on ER%, whereas eluent volume has net positive effect.

$$ER\%_{MG} = 153.0 - 134.3\,X_1 + 0.5\,X_2 - 8.1\,X_3 + 0.3\,X_1X_2 + 10.7\,X_1X_3 + 0.04\,X_2X_3 - 0.004\,X_2^2 - 0.54X_3^2 \quad (7)$$

From the ANOVA study, the "lack of fit F-value" of 6.027 proof it is not significant relative to the pure error and show that no-significant lack of fit was signified for the ER% [41] and also reveal the validity of quadratic model for predication of result of present study.[17, 34, 42] The model F-value of 301.020 implies that the model was significant (Table 4).

There was only a 0.01% chance that model F-value is due to noise. The F-value (301.020) of model with low probability ($p < 0.0001$) justify the model significancy. The goodness of fit was also evidenced by the correlation coefficient (R^2; Table 3). The R^2 value of 0.997 show that more than 99.7% of the data deviation could be explained by the developed quadratic model and the predicted R^2 values has good agreement with adjusted R^2 and suggest all terms depicted in the model were significant. The R^2 value indicate that only 0.003% of the total variable was not explained by the model. The reproducible and repeatable coefficient of variance (CV%) as ratio of the standard error to the mean response value of is not greater than 10% and show acceptable predicated results.

According to Table 3, the CV% values obtained for response studied are relatively smaller than 2.40%. The adequate precision (AP) ratio of the models for MG ER% was 60.30 that is adequate model signal. AP values higher than 4 are desirable and confirm that the constructed models is applicable to navigate the space defined by the CCD.[43] Plot of observed that versus those obtained from Eq. (7) is shown in Fig. 5A. The figure proves that the predicted response from the empirical model has good agreement with the observed data. Fig. 5B depicts the diagram of the residuals based on the predicted response percent efficiency. No evident process is supposed to be observed in this diagram.

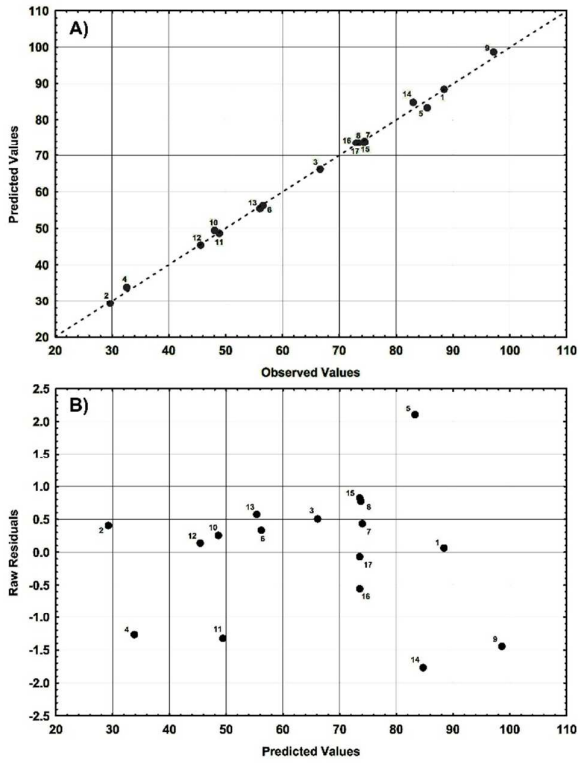

Fig. 5. A) Plot of observed value vs. predicted value for extraction recovery of MG. B) Plot of predicted value versus residuals for extraction recovery of MG.

3.4. Response surface methodology

The surface response plot show the effect of eluent volume and amount of sorbent has significant influence on MG ER%. Sorbent value show negative linear effect and positive quadratic effect on the ER% ($p< 0.00016$; $p< 0.896$). Eluent volume has positive linear effect and negative quadratic effect on the extraction efficiency ($p< 0.025$; $p< 0.0005$). The ER% firstly increased and subsequently, raising the volume of eluent lead to reduce in ER%. 120 µL of eluent is favourable for obtaining high ER% at lower sorbent mass. It was observed that the extraction recovery decrease with increasing the amount of sorbent and/or volume of extraction solvent.

Figure 6(B) shows the variation in ER% with eluent volume and pH. Eluent volume has a negative effect on recovery at constant rate of pH.

Fig. 6A–B, in the middle value of eluent volume with respect to the axial ER%, suggest slightly increases and subsequent reaching a plateau. In general a view glance to the results reveal that the efficiency of extraction was increased and reach constant at 0.5-0.8 mg, 5-8 and 80-140 µL for amount of sorbent, pH and eluent volume, respectively.

3.5. Optimization of CCD by DF

Numerical optimization is based on selection by proper value of minimum and maximum of each parameter. Optimization of three objectives namely mass of sorbent, eluent volume and pH influence was examined and their response, is shown in Fig. 6C. In this figure, the lines illustrate the ranges of parameters obtained from the model, with the exact quantity of each parameter shown by the circles. The bottom lines show the variation of MG ER% with respect to the model parameters. A vertical line (Fig. 6C) show that mass of sorbent, eluent volume and pH have optimum point at 0.6 mg, 120 µL at pH=6.0 that cause maximum ER% of 97.15% with desirability of 1.00. Based on the desirability plot, maximum removal of 97.40%) were obtained following the replication of similar experiments (N=3) at optimum conditions.

3.6. Analytical performance of the DNSPME

To evaluate the practical applicability of this method, several characteristics properties like detection limit, linear range, precision and relative standard deviation under the optimized conditions were investigated and compared with literature (Tables 5 and 6). Table 5 shows that under study method has linear calibration curve over the concentration range of 1-4000 ng mL^{-1} with determination coefficient (R^2) of 0.999. The limit of detection ($3S_b/m$) and limit of quantification ($10S_b/m$), calculated as three and ten times the standard deviation (S_b) of the blank signal divided by the calibration curve slope (m), were found to be 0.175 ng mL^{-1} and 0.583 ng mL^{-1}, respectively. The relative standard deviation (RSD %, N=3), has value in the range of 2.8% - 4.5% with in different real samples, while the enhancement factor is 43.54 and recoveries between 90.28–97.93%.

A comparison of the presented method with literature for MG determination is shown in Table 6. As can be seen, the RSD, LOD, LOQ, Linear range and relative recovery of the presented method are superior to other reported methods. As it can be seen, the analytical performance of the proposed DNSPME system is similar to or better than the miniaturized extraction methods described in the literature. The method is able to by consumption of very low quantity of sorbent (0.6 mg) in short time (<5 min) accumulate on magnetic γ-Fe_2O_3-NPs-AC that simply phase separation occur through exposure to magnetic field.

New Journal of Chemistry

ARTICLE

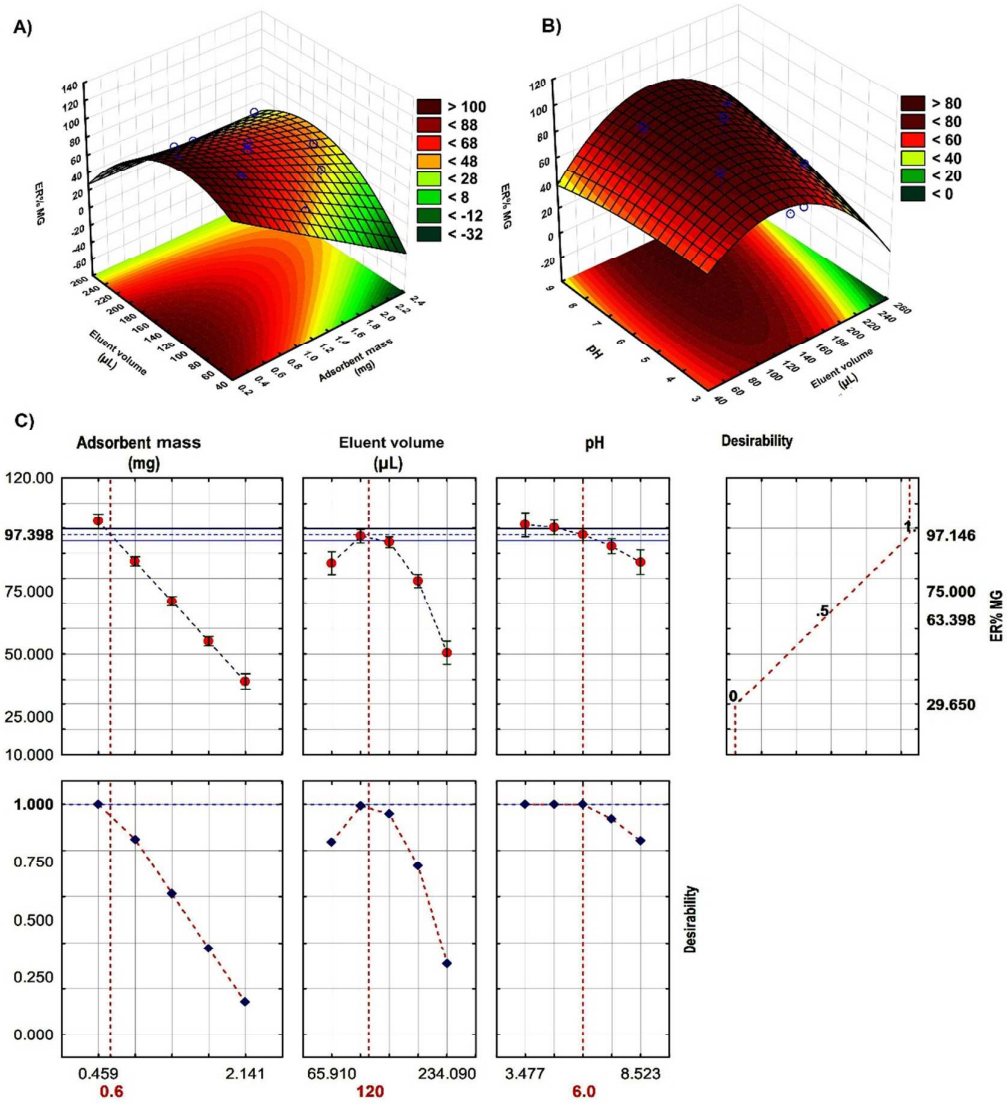

Fig. 6. Response surfaces for the 2^3 central composite designs: A) Eluent volume (µL)-adsorbent mass (mg), B) pH- Eluent volume (µL) and C) Profiles for predicated values and desirability function for extraction recovery of MG. Dashed line indicated current values after optimization.

Table. 5 Analytical characteristics of the proposed DNSPME method.

Quantitative analysis		
Regression equation before preconcentration	y = 0.193x - 0.009,	R^2 = 0.999
Regression equation after preconcentration	y = 8.388x - 0.039,	R^2 = 0.999
Sample volume (mL)	10	
Volume eluent solvent (µL)	120	
Linear range (ng mL^{-1})	1-4000	
Limit of detection (LOD) (ng mL^{-1})	0.175	
Reproducibility (RSD, %)	2.587 - 4.454	

Repeatability (RSD, %) (N=10)	2.790
Average recoveries (%) in samples at spiked	94.836
Limit of quantification (LOQ) (ng mL^{-1})	0.583
Preconcentration factor	83.333
Enrichment factor	43.542

Table. 6 Comparison of the published methods with the proposed method in this work.

Method	Correlation coefficient	Relative recovery (%)	Precision (% RSD)	LOD (ng mL^{-1})	LOQ (ng mL^{-1})	Linear range (ng mL^{-1})	Ref.
HPLC [a]	0.9998	88.7-113.9	≤10	1.23	4.100	10-600	20
HPLC-FD [b]	0.9997	87.4-94.6	4.5–5.9	0.05	0.167	5-500	44
LC [c]	-	85-95	3.9-7.0	-	-	25- 250	45
EUPLC-TMS [d]	-	78.4-90.3	3.7-5.8	0.18-0.48	0.60-1.60	0.5-1000	9
UPLC-ESI-MS /MS [e]	-	85.3-104.4	<15	0.270	1.00	0.25-20.0	10
HPLC [a]	0.9875	76.8–93.7	2.12-10.09	-	-	500-1800	21
LC-LIT-MS/MS [f]	0.9937	85-98	12	0.003-0.02	0.005-0.025	1-100	6
UPLC-ESI-MS /MS [e]	0.9990	82.7-103.4	3.94-5.18	1.5	5.00	0.25-50	11
LC [c]	0.9994	76.7–82.3	3.2-4.6	0.01	0.03	20-10000	46
LC-TMS [g]	0.9991	82.1-102.9	8-13	-	-	0.1-10	7
HPLC [a]	0.9997	89.8- 99.1	4.9-7.2	-	-	10.0-250	47
LC-MS/MS [h]	0.9976	71.2–112.6	0.6-9.1	0.1-1.0	1-3.3	0.1-2.0	8
LC-VIS/FLD [i]	0.9999	60.4-63.5	7.7-10.9	0.15	0.37	0–100	2
ECL-MISPE [j]	0.9956	84.5-96.6	5.6-14.5	1.1	3.65	0.02-5	13
UHPLC-MS/MS [k]	0.9900	48–95	≤24	0.05-0.20	0.2-0.5	1–250	12
LC-TMS [g]	0.9990	81-98	<7.6	0.10	0.29	0.005-0.5	3
Spectrophotometric	0.9989	89-106	8.1	1.4	4.7	10-1000	14
Spectrophotometric	0.9968	59.4-94.3	2.2-5.3	67	224	0.21-8.0	15
Spectrophotometric	0.9991	92.5-104	≤5.4	0.28	0.984	0.50-250	16
Spectrophotometric	0.9998	90.3-97.90	2.79-4.45	0.175	0.584	1-4000	This work

[a] High Performance Liquid Chromatographic
[b] High Performance Liquid Chromatographic with Fluorescence Detection
[c] Liquid Chromatographic
[d] Extraction-Ultra Performance Liquid Chromatography-Tandem Mass Spectrometry
[e] Ultra-High Performance Liquid Chromatography-Electrospray Ionization Tandem Mass Spectrometry
[f] Liquid Chromatography-Linear Ion Trap Mass Spectrometry
[g] Liquid Chromatography-Tandem Mass Spectrometry
[h] Liquid Chromatography-Mass Spectrometry
[i] Liquid Chromatography with Visible and Fluorescence Detection
[j] Electro-Chemi-Luminescence (ECL) inhibition method combined with Molecularly Imprinted Solid Phase Extraction (MISPE)
[k] Ultra-High Performance Liquid Chromatography-Tandem Mass Spectrometry

3.7. Real sample analysis

The present DNSPME methods was applied for MG determination in distilled, tap, mineral, rain, river, trout fish water and wastewater samples under previously optimized point (Table 7). Water samples were filtrated to remove sediments or particles. Then the sample was stored in bottles when the analysis of water samples was not immediately carried out. The storage period was kept as short as possible. In the water samples and trout fish no MG was detected. Then trout fish and water samples were spiked under the optimum conditions established above. The relative recovery of MG from above mention samples following at spiking with 600 ng mL^{-1} (Table 7) was more than 90.0% with RSD lower than 5.0%. In this case, the recoveries are slightly lower for river and wastewaters than for the other matrices that reflect their very salinity nature.

4. Conclusion

In the present study, a new dispersive-nanoparticles-solid phase microextraction method based on nanoparticles as stationary phases combined with spectrophotometric was developed for MG quantification in different water samples. For this purpose, a Plackett-Burman design was applied for this study to understand the most influencing variables and subsequently Central Composite Design for optimizing the significant factors. The optimal conditions for ER% were set as sorbent mass of 0.6 mg, eluent volume 120 µL, and pH 6.0. Under the optimized conditions, the maximum ER% of MG achieved was 97.9%. Accordingly, this method possesses great potential in the analysis of MG in water samples, Also in comparison with other literatures (Table 6), this sorbent and method have shown good advantages.

Table.7 Extraction recoveries and RSD in different water samples at spiked level by the DNSPME method (N=3).

Samples	Added (ng mL^{-1})	Found (ng mL^{-1})	ER% ± RSD (%)

Double-distilled water	600	587.579	97.930±3.307[a]
Mineral water [b]	600	561.232	93.539±3.677
Tap water [c]	600	574.355	95.726±2.587
Rain water	600	582.417	97.069±2.753
River water [d]	600	551.573	91.929±2.841
Wastewater [e]	600	541.705	90.284±4.454
Trout fish water [f]	600	584.240	97.373±2.841

[a] Mean value ± RSD.

[b] Zamzam mineral water, Isfahan, Iran

[c] From drinking water system of Yasouj, Iran

[d] From Beshar river, Yasouj, Iran

[e] From Yasouj, Iran

[f] Sample was taken from fish water in Yasouj, Iran.

Water samples without spiking was used as blank.

Acknowledgement

The author expresses their appreciation to the Yasouj University, Yasouj, Iran for financial support of this work.

References

1 K. Halme, E. Lindfors and K. Peltonen, *Food Addit. Contam.*, 2004, **21**, 641-648.
2 K. Mitrowska, A. Posyniak and J. Zmudzki, *J. Chromatogr. A*, 2005, **1089**, 187-192.
3 J. M. Van de Riet, C. J. Murphy, J. N. Pearce, R. A. Potter and B. G. Burns, *J. AOAC Int.*, 2005, **88**, 744-749.
4 S. J. Culp and F. A. Beland, *Int. J. Toxicol.*, 1996, **15**, 219-238.
5 S. Srivastava, R. Sinha and D. Roy, *Aquatic toxicol.*, 2004, **66**, 319-329.
6 M. J. M. Bueno, S. Herrera, A. Uclés, A. Agüera, M. D. Hernando, O. Shimelis, M. Rudolfsson and A. R. Fernández-Alba, *Anal. Chim. Acta*, 2010, **665**, 47-54.
7 Y. Tao, D. Chen, X. Chao, H. Yu, P. Yuanhu, Z. Liu, L. Huang, Y. Wang and Z. Yuan, *Food Control*, 2011, **22**, 1246-1252.
8 L. Guo, J. Zhang, H. Wei, W. Lai, Z. P. Aguilar, H. Xu and Y. Xiong, *Talanta*, 2012, **97**, 336-342.
9 Z.-L. Zhang, P. Zhang and D.-Z. Shen, *Fenxi Huaxue*, 2012, **40**, 487-488.
10 Y. m. Guang. ming , Chen. Xue-chang, Zhang. Xiao-jun, LI. Pei, HE. Yina. , *Chinese J. Anal. Lab.*, 2013, **08**, 657-663.
11 L. Chen, Y. Lu, S. Li, X. Lin, Z. Xu and Z. Dai, *Food chem.*, 2013, **141**, 1383-1389.
12 N. López-Gutiérrez, R. Romero-González, P. Plaza-Bolaños, J. L. Martínez-Vidal and A. Garrido-Frenich, *Food Anal. Methods*, 2013, **6**, 406-414.
13 Z. Guo, P. Gai, T. Hao, J. Duan and S. Wang, *J. Agric. Food. Chem.*, 2011, **59**, 5257-5262.
14 P. Richter, A. Cañas, C. Muñoz, C. Leiva and I. Ahumada, *Anal. Chim. Acta*, 2011, **695**, 73-76.
15 Y. S. Al-Degs and J. A. Sweileh, *Arabian J. Chem.*, 2012, **5**, 219-224.
16 A. Afkhami, R. Moosavi and T. Madrakian, *Talanta*, 2010, **82**, 785-789.
17 A. A. Asgharinezhad, H. Ebrahimzadeh, F. Mirbabaei, N. Mollazadeh and N. Shekari, *Anal. Chim. Acta*, 2014, **844**, 80-89.
18 M. Ghaedi, G. Negintaji and F. Marahel, *J. Ind. Eng. Chem.*, 2014, **20**, 1444-1452.
19 Z. Zhang, H. Zhang, Y. Hu and S. Yao, *Anal. Chim. Acta*, 2010, **661**, 173-180.
20 M. Hu, J. Chen, J. H. Yang, Y. P. Zhang, X. M. Zhou and L. Y. Bai, *J. Chinese Chem. Soc.*, 2015, **62**, 305-310.
21 Y.-h. Li, T. Yang, X.-l. Qi, Y.-w. Qiao and A.-p. Deng, *Anal. Chim. Acta*, 2008, **624**, 317-325.
22 G. A. Ozin, A. C. Arsenault and L. Cademartiri, *Nanochemistry: a chemical approach to nanomaterials*, Royal Society of Chemistry, 2009.
23 S. Laurent, D. Forge, M. Port, A. Roch, C. Robic, L. Vander Elst and R. N. Muller, *Chem. Rev.*, 2008, **108**, 2064-2110.
24 S. Laurent, D. Forge, M. Port, A. Roch, C. Robic, L. Vander Elst and R. N. Muller, *Chem. Rev.*, 2009, **110**, 2574-2574.
25 E. Darezereshki, M. Ranjbar and F. Bakhtiari, *J. Alloys Compd.*, 2010, **502**, 257-260.
26 A. Asfaram, M. Ghaedi, A. Goudarzi and M. Soylak, *RSC Adv.*, 2015, **5**, 39084-39096.
27 M. Roosta, M. Ghaedi, A. Daneshfar and R. Sahraei, *J. Chromatogr. B*, 2015, **975**, 34-39.
28 R. L. Plackett and J. P. Burman, *Biometrika*, 1946, 305-325.
29 W.-H. Chung, S.-H. Tzing and W.-H. Ding, *J. Chromatogr. A*, 2013, **1307**, 34-40.
30 M. Rezaee, Y. Yamini and M. Faraji, *J. Chromatogr. A*, 2010, **1217**, 2342-2357.
31 S. Khodadoust, M. S. Talebianpoor and M. Ghaedi, *J. Sep. Sci.*, 2014, **37**, 3117-3124.
32 J. He, Q. Zhen, N. Qiu, Z. Liu, B. Wang, Z. Shao and Z. Yu, *Bioresour. Technol.*, 2009, **100**, 5922-5927.
33 G. E. Box and K. Wilson, *J. R. Stat. Soc. Series B,* 1951, **13**, 1-45.
34 K. Ahmadi, Y. Abdollahzadeh, M. Asadollahzadeh, A. Hemmati, H. Tavakoli and R. Torkaman, *Talanta*, 2015, **137**, 167-173.
35 S. Khodadoust and M. Ghaedi, *J. Sep. Sci.*, 2013, **36**, 1734-1742.
36 A. Goudarzi, A. D. Namghi and C.-S. Ha, *RSC Adv.*, 2014, **4**, 59764-59771.
37 S. K. Bhar, N. Mukherjee, S. K. Maji, B. Adhikary and A. Mondal, *Mater. Res. Bull.*, 2010, **45**, 1948-1953.
38 P. Saravanan, J.-H. Hsu, D. Sivaprahasam and S. Kamat, *J. Magn. Magn. Mater.*, 2013, **346**, 175-177.
39 A. K. Dutta, S. K. Maji and B. Adhikary, *Mater. Res. Bull.*, 2014, **49**, 28-34.
40 S. Sahoo, K. Agarwal, A. Singh, B. Polke and K. Raha, *Int. J. Eng. Sci. Technol.*, 2010, **2**, 118-126.
41 M. A. Bezerra, R. E. Santelli, E. P. Oliveira, L. S. Villar and L. A. Escaleira, *Talanta*, 2008, **76**, 965-977.
42 H. Ebrahimzadeh, N. Tavassoli, O. Sadeghi and M. M. Amini, *Talanta*, 2012, **97**, 211-217.
43 M. J. Bashir, H. A. Aziz, M. S. Yusoff and M. N. Adlan, *Desalination*, 2010, **254**, 154-161.
44 J.-c. DENG, L.-h. LI, X.-q. YANG, J.-w. CEN, S.-p. XIN, Y. WEI and Y.-y. WU, *Food Sci.*, 2012, **14**, 033.
45 S. M. Plakas, K. R. El Said, G. R. Stehly and J. E. Roybal, *J. AOAC Int.*, 1994, **78**, 1388-1394.
46 H. Sun, L. Wang, X. Qin and X. Ge, *Environ. Monit. Assess.*, 2011, **179**, 421-429.
47 C. Long, Z. Mai, Y. Yang, B. Zhu, X. Xu, L. Lu and X. Zou, *J. Chromatogr. A*, 2009, **1216**, 2275-2281.

The paper presents an extraction method based on dispersive-nanoparticles-solid phase microextraction for preliminary preconcentration and subsequent spectrophotometric determination of trace amounts of malachite green.